Published in final edited form as:
Neuroscience. 2008 August 26; 155(3): 818–832. doi:10.1016/j.neuroscience.2008.05.037.

Localization of electrogenic Na/bicarbonate cotransporter NBCe1 variants in rat brain

Debeshi Majumdar[1], **Arvid B. Maunsbach**[2], **John J. Shacka**[3], **Jennifer B. Williams**[1], **Urs V. Berger**[4], **Kevin P. Schultz**[1], **Lualhati E. Harkins**[5], **Walter F. Boron**[6], **Kevin A. Roth**[3], and **Mark O. Bevensee**[1,7,8]

[1]Department of Physiology and Biophysics, University of Alabama at Birmingham, Birmingham, AL 35294

[2]The Water and Salt Research Center, Institute of Anatomy, University of Aarhus, DK-8000 Aarhus C, Denmark

[3]Department of Pathology, Division of Neuropathology, University of Alabama at Birmingham, Birmingham, AL 35294

[4]UB In Situ, Natick, MA 01760

[5]Surgical Service, Birmingham Veterans Affairs Hospital, Birmingham, AL 35294

[6]Department of Physiology and Biophysics, Case Western Reserve University, Cleveland, OH 44106

[7]Center of Glial Biology in Medicine, University of Alabama at Birmingham, Birmingham, AL 35294

[8]Civitan International Research Center, University of Alabama at Birmingham, Birmingham, AL 35294

Abstract

The activity of HCO_3^- transporters contributes to the acid-base environment of the nervous system. In the present study, we used *in situ* hybridization, immunoblotting, immunohistochemistry, and immunogold electron microscopy to localize electrogenic Na/bicarbonate cotransporter NBCe1 splice variants (-A, -B, and -C) in rat brain. The *in situ* hybridization data are consistent with NBCe1-B and -C, but not -A, being the predominant NBCe1 variants in brain, particularly in the cerebellum, hippocampus, piriform cortex, and olfactory bulb. An antisense probe to the B and C variants strongly labeled granule neurons in the dentate gyrus of the hippocampus, and cells in the granule layer and Purkinje layer (e.g., Bergmann glia) of the cerebellum. Weaker labeling was observed in the pyramidal layer of the hippocampus and in astrocytes throughout the brain. Similar, but weaker labeling was obtained with an antisense probe to the A and B variants. In immunoblot studies, antibodies to the A and B variants (αA/B) and C variant (αC) labeled ~130-kDa proteins in various brain regions. From immunohistochemistry data, both αA/B and αC exhibited diffuse labeling throughout brain, but αA/B labeling was more intracellular and punctate. Based on co-localization

Address correspondence to: Mark O. Bevensee, PhD, Department of Physiology and Biophysics, University of Alabama at Birmingham, 1918 University Blvd., 812 MCLM, Birmingham, AL 35294, Ph: (205) 975-9084; Fax: (205) 975-7679, E-mail: E-mail: bevensee@physiology.uab.edu.

Section Editor: Dr. Charles R. Gerfen (Neuroanatomy)

studies with antibodies to neuronal or astrocytic markers, αA/B labeled neurons in the pyramidal layer and dentate gyrus of the hippocampus, as well as cortex. αC labeled glia surrounding neurons (and possibly neurons) in the neuropil of the Purkinje cell layer of the cerebellum, the pyramidal cell layer and dentate gyrus of the hippocampus, and the cortex. According to electron microscopy data from the cerebellum, αA/B primarily labeled neurons intracellularly and αC labeled astrocytes at the plasma membrane. In summary, the B and C variants are the predominant NBCe1 variants in rat brain and exhibit different localization profiles.

Keywords

cerebellum; glia; hippocampus; neuron; pH; transporter

INTRODUCTION

It is well established that pH is an important cellular parameter because alterations in pH can affect a variety of cellular processes including the activity of enzymes and ion channels. In the nervous system, changes in pH can influence neuronal activity. In general, a decrease in extracellular pH (pH_o)inhibits neuronal activity, whereas an increase in pH stimulates activity (Chesler and Kaila, 1992; Ransom, 2000; McAlear and Bevensee, 2003; Chesler, 2003). Changes in pH are also seen with neuropathologic conditions. For example, decreases in brain pH are associated with ischemia, hypoxia, and epileptic events leading to neuronal necrosis and overall brain damage (Katsura and Siesjo, 1998).

The regulation of brain pH is complex because the movement of acid-base equivalents across the plasma membranes of neurons and glia (e.g. astrocytes and oligodendrocytes) changes both pH_o and the intracellular pH (pH_i) of cells. Cells use a system of acid-base transporters in their plasma membranes to regulate pH_i, and subsequently pH_o. Some of the most powerful acid-base transporters in brain cells include HCO_3^--dependent ones, which are now classified as members of a bicarbonate transporter (BT) superfamily following their molecular identification over the past decade (Romero et al., 2004). The BT superfamily is comprised of anion exchangers (AEs), electrogenic and electroneutral Na/bicarbonate cotransporters (NBCs), and Na-driven Cl-bicarbonate exchangers (NDCBEs).

The role of an electrogenic NBC in the nervous system has received considerable attention because the transporter couples changes in pH with neuronal activity (Chesler, 2003). In the nervous system, the activity of an electrogenic NBC was first characterized in invertebrate leech glial cells (Deitmer and Schlue, 1987; Deitmer and Schlue, 1989; Deitmer, 1992), and subsequently identified in a number of mammalian astrocytes (see (Rose and Ransom, 1998; McAlear and Bevensee, 2003)). In at least rat hippocampal astrocytes, the transporter has a stoichiometry of 1 Na^+:2 HCO_3^-(Bevensee et al., 1997a; Bevensee et al., 1997b) and functions as an acid extruder. According to the model proposed by Chesler (Chesler, 1990) and Ransom (Ransom, 1992), astrocytes modulate neuronal excitability through NBC-mediated changes in pH_o. More specifically, an elevation in extracellular K^+ (K^+_o) during neuronal activity depolarizes astrocytes, thereby stimulating electrogenic NBC activity to transport Na^+, HCO_3^-, and net negative charge into the astrocytes. The ensuing decrease in pH_o will tend to dampen further neuronal activity. In support of this model, high K^+_o depolarizes astrocytes in the gliotic hippocampal slice and elicits a Na^+- and HCO_3^--dependent decrease in pH_o due to the activity of an NBC (Grichtchenko and Chesler, 1994a; Grichtchenko and Chesler, 1994b).

Our understanding of NBCs in the brain has advanced with the molecular identification of cDNAs encoding variants of electrogenic NBCs (NBCe1 and NBCe2) and electroneutral NBCs

(NBCn1). NBCe1 —the first NBC to be cloned (Romero et al., 1997)— has three splice variants: NBCe1-A, -B, and -C (Romero et al., 2004). In early cloning studies, the A variant was identified in rat and human kidney (Burnham et al., 1997; Romero et al., 1998), the B variant in human heart (Choi et al., 1999), human pancreas (Abuladze et al., 1998a), and rat brain (Bevensee et al., 2000), and the C variant in rat brain (Bevensee et al., 2000). These three variants are identical to one another except at the amino and/or carboxy termini. The amino-terminal 85 residues of the B and C variants replace 41 residues of the A variant, whereas the carboxy-terminal 61 residues of the C variant replace 46 residues of the A and B variants. This C variant —found predominantly in brain (Bevensee et al., 2000)— arises from a 97-base pair deletion near the 3′ ORF, thereby shifting the stop codon further 3′.

Shortly after NBCe1 was identified, two groups (Schmitt et al., 2000; Giffard et al., 2000) examined the localization of NBCe1 in rat brain primarily using polynucleotide probes and/or polyclonal antibodies that did not distinguish among the three splice variants. Somewhat expectedly, both groups found NBCe1 widely distributed throughout the brain and localized to glial cells. However, a surprise finding was the presence of NBCe1 in some neuronal populations, including granule cells of the hippocampus and neurons of the cortex (Schmitt et al., 2000).

Clearly, it would be informative to know which of the three NBCe1 variants are expressed in brain, and in what cell types. In the aforementioned Giffard *et al.* study on rat brain (Giffard et al., 2000), the authors briefly noted that *in situ* hybridization with the nonspecific NBCe1 probe was mimicked by a more specific probe to the B and C variants, but not by a probe to the A variant, which displayed minimal labeling. Somewhat surprisingly, Rickmann *et al.* (Rickmann et al., 2007) recently reported the expression of both NBCe1-A and NBCe1-B in mouse brain based on immunohistochemistry and immunoelectron microscopy. The authors found expression of the A variant throughout brain, particularly in neuronal subpopulations in the cerebellum, hippocampus, cerebral cortex, and olfactory bulb. In contrast, the authors reported the expression of NBCe1-B in astroglia and Bergmann glia. However, it is important to point out that the NBCe1-B antibody is expected to recognize not only NBCe1-B, but also NBCe1-C, which is predominately expressed in brain of at least rat. Therefore, the expression profiles of the B and C variants in brain have yet to be eludicated.

In the present study, we used mRNA and protein localization techniques to examine all three NBCe1 splice variants in rat brain. According to *in situ* hybridization data, NBCe1-A mRNA is minimal in brain, whereas NBCe1-B and possibly -C mRNAs are predominantly found in cerebellum (granule and Purkinje layers), hippocampus (dentate gyrus and pyramidal layers), piriform cortex, and olfactory bulb. In immunoblot studies, we used previously characterized antibodies (Bevensee et al., 2000) that distinguish between the C terminus of either the C variant (αC) or the A/B variant (αA/B). Both antibodies recognized a ~130-kDa protein from all brain regions. Based on immunohistochemistry studies, αA/B displayed weak diffuse labeling throughout the brain and punctate labeling of pyramidal neurons in the hippocampus and neurons in the cortex. In contrast, αC displayed stronger diffuse labeling throughout the brain. αC appeared to label glia more so than the surrounding neurons in the cerebellum, hippocampus, and cortex. Immunoelectron microscopy data from the cerebellum support the plasma-membrane expression of NBCe1-C in astrocytes and intracellular expression of NBCe1-B in neurons. Portions of this work have been published in abstract form (Majumdar et al., 2006).

EXPERIMENTAL PROCEDURES

Animals

All animals were housed in approved animal care facilities at the University of Alabama at Birmingham (UAB). The animal facilities are under the direction of full-time veterinarians and are fully accredited by the American Association for Accreditation of Laboratory Animal Care, and meet all standards prescribed by the "Guide for the Care and Use of Laboratory Animals". All protocols involving animals were approved by the Institutional Animal Care and Use Committee at UAB.

In situ hybridization

Designing NBC probes—Sense and antisense probes were created by PCR using primers that flanked the following regions: *i*) the unique 5' open reading frame (ORF) encoding the unique amino-terminal 41 residues of the A variant, *ii*) the different 5' ORF encoding the different amino-terminal 85 residues of the B and C variants, and *iii*) the 97-bp region near the 3' end of the ORF found exclusively in the A and B variants (Fig. 1). PCR products were purified and directionally subcloned into PCRII TOPO® vector (Invitrogen, Inc.). cRNA probes were generated by transcription using the T7 or SP6 promoter.

Performing in situ hybridization—Non-radioactive *in situ* hybridization was performed as previously described using digoxigenin (DIG)-labeled cRNA probes (Berger and Hediger, 2001). Frozen rat brain or kidney sections (10 μm), were captured onto Superfrost plus microscope slides (Fisher Scientific, Pittsburgh, PA). Sections were fixed, acetylated, and incubated in the NBC probes (~100 ng/ml) at 70°C for three days. Hybridized probes were visualized using alkaline phosphatase-conjugated anti-DIG Fab fragments (Roche, Indianapolis, IN) and 5-bromo-4-chloro-3-indolyl-phosphate/nitro blue tetrazolium substrate (Kierkegard and Perry Laboratories, Gaithersburg, MD). Sections were rinsed several times in a pH-9.5 solution containing 150 mM NaCl, 100 mM Tris, and 20 mM EDTA, and then coverslipped with glycerol gelatin. Control sections were incubated in the same concentration of the sense probe.

Immunoblotting

NBCe1 antibodies—Previously characterized polyclonal antibodies (Bevensee et al., 2000) distinguish between the C terminus of either the C variant (αC) or the A/B variant (αA/B) (Fig. 1). αA/B and αC labeling are specific based on competition immunoblot experiments whereby antibody labeling of microsomal protein from total rat brain or oocytes injected with a cDNA encoding an NBCe1 variant was inhibited by preabsorbing the antibodies with the corresponding antigenic fusion protein (Bevensee et al., 2000; Williams and Bevensee, unpublished data).

Labeling protein from rat brain regions—We used two commercially available adult rat brain blots (Chemicon International, Inc., Temecula, CA) containing ~25-30 μg protein from different brain regions of Sprague-Dawley 12-16 wk-old male rats (~150 g). The membranes were preincubated in BLOTTO (1× PBS + 5% dry-milk powder + 0.05% Tween-20) for 30 min, and then BLOTTO containing either 1:500 rabbit αA/B, 1:2K rabbit αC, or 1:5K mouse αβ-actin (Sigma-Aldrich, St. Louis, MO) for 1 h. Membranes were subsequently incubated in BLOTTO containing HRP-conjugated secondary anti-IgG (Jackson ImmunoResearch Laboratories, Inc., West Grove, PA) for 1 h. Labeling was detected using the SuperSignal West Pico chemiluminescence kit (Pierce Biotechnology, Inc., Rockford, IL) and recorded by exposure to HXR film (Hawkins X-Ray Supply, Oneonta, AL). The blot was stripped of bound antibody by first incubating the membrane in stripping buffer (100 mM β-mercaptoethanol,

2% SDS, 62.5 mM Tris-HCl, pH ~6.8) at 50°C for 30 min with occasional rocking, and then washing the membrane in PBS containing 0.05% Tween-20.

Densitometry analysis was performed using Biorad Quantity One software (version 4.5.1).

Immunohistochemistry

Antibody labeling—Excised brains from adult male Sprague-Dawley rats were fixed in Bouin's fixative (71% saturated picric acid, 24% formalin, and 5% glacial acetic acid) overnight at 4°C, and then rinsed with 70% ethanol (or 67% ethanol/3.5% isopropanol). The brains were subsequently incubated in 70% ethanol (or 67% ethanol/3.5% isopropanol) for at least 6 h at 4°C before being embedded in paraffin. 5-μm sagittal or coronal sections were cut using a HM 355S microtome (Richard-Allan Scientific, Kalamazoo, MI) and mounted onto glass slides. Sections were de-paraffinized by incubating the sections first in Citrisolv® (Fisher Scientific) for 5 and 10 minutes, and then in isopropanol (Fisher Scientific) 3×5 min. For optimal αC labeling, the sections were then subjected to an antigen-retrieval protocol, which involved incubating the sections in a 10 mM citrate buffer (pH 6.0) in a steam-set rice cooker for 30 min. Sections were then oxidized with 3% H_2O_2 for 10 min at room temperature (RT) to remove endogenous peroxidase activity. For optimal αA/B labeling, antigen retrieval was not required.

For antibody labeling, sections were incubated first in a blocking buffer containing PBS supplemented with 1% BSA (Fisher Scientific), 0.2% evaporated milk (Nestle, Solon, OH), and 0.3% Triton X-100 for 15 min at RT, and then in the blocking buffer with primary antibody overnight at 4°C. In competition experiments, fusion protein was added to the blocking buffer plus primary antibody and rocked for 1 h at RT before the buffer was applied to sections overnight. Sections were next washed with 1× PBS, and then incubated in blocking buffering containing 1:1K or 1:2K HRP-conjugated donkey anti-rabbit, donkey anti-mouse, or donkey anti-guinea pig antibody (Jackson Labs) for 1 h at RT. Labeling was detected using tyramide signal amplification, which involved incubating sections in a 1:500 dilution of Cy3- or FITC-conjugated tyramide dissolved in Plus Amp buffer (PerkinElmer LAS, Inc., Boston, MA) for 30 min at RT. Sections were next labeled with 0.2 μg/ml bis benzimide (Hoechst 33,258) nuclear counter stain for 10 min. The slides were coverslipped using 1:1 PBS:glycerol.

In negative controls, labeling was very weak in the absence of primary antibody. For double antibody labeling protocols, results were similar regardless of the order of antibody labeling. A relative lack of residual HRP activity remaining from the first round of labeling was confirmed in control studies where the second primary antibody was omitted. All immunohistochemical labeling was performed a minimum of two times.

Additional antibodies used in this study were anti-mouse neuronal nuclei (NeuN) (Chemicon), anti-mouse microtubule-associated protein (MAP2) (Sigma-Aldrich), anti-mouse Calbindin (Sigma-Aldrich), GFAP (Chemicon), GLAST (Chemicon), and anti-mouse β1 of the Na^+ pump (Upstate Biotechnology, Inc. Lake Placid, NY).

Visualizing antibody labeling—For some images, antibody labeling of sections was examined with an Axioskop microscope (Zeiss, Thornwood, NY) equipped with epifluorescence capabilities, and images were captured using Axiovision® software. For other images, antibody labeling was examined with a Leica inverted DMIRBE confocal microscope (High Resolution Imaging Facility, University of Alabama at Birmingham). The following excitation lasers were used: *i*) Argon (488 nm) for FITC (green), *ii*) Krypton (568 nm) for Cy3 (red), and *iii*) UV (351 nm) for nuclear labeling (blue).

Electron Microscopy

Four rats (230–300 g) were anesthetized by halothane (Halocarbon, River Edge, NJ) and perfusion-fixed through the heart for 3 min with a 4% paraformaldehyde (PFA) solution containing 0.1 M sodium cacodylate buffer (pH 7.2). The initial perfusion rate was ~230 ml/min. The brains were excised and post-fixed in the same fixative for 4 h. Small tissue blocks were trimmed from the cerebellum, rinsed in buffer, infiltrated with 2.3 M sucrose, mounted on holders, and frozen in liquid nitrogen. The tissue was then cryosubstituted in a Reichert AFS freeze-substitution apparatus (Leica, Germany) and embedded in Lowicryl HM20 as previously described (Maunsbach et al. 2000). Briefly, samples were sequentially equilibrated over three days in methanol containing 0.5% uranyl acetate at temperatures gradually increasing from −90°C to −70°C, rinsed in pure methanol, infiltrated with Lowicryl HM20 at −45°C, and finally, UV-polymerized for two days at −45°C and two days at 0°C. Ultrathin Lowicryl sections were cut at ambient temperature on a Leica Reichert Ultracut S ultramicrotome (Leica, Vienna, Austria) and first blocked by incubation in PBS containing 0.05 M glycine and 0.1% skimmed milk powder. The sections were then incubated overnight at 4°C with 1:100 αC or 1:25 αA/B in PBS containing 0.1% skimmed milk powder. The primary antibodies were visualized using goat anti-rabbit IgG conjugated to 10-nm colloidal gold particles (GAR.EM1O, BioCell Research Laboratories, Cardiff, UK) diluted 1:50 in PBS with 0.1% skimmed milk powder and polyethyleneglycol (5 mg/ml). The sections were stained with uranyl acetate and lead citrate before examination with a Morgagni electron microscope (Eindhoven, The Netherlands). Immunolabeling controls consisted of replacing the primary-antibody serum with either pre-immune rabbit IgG or preabsorbed antibody serum containing the appropriate maltose binding protein (MBP)-fusion protein used to generate the antibody. All controls showed absence of specific labeling.

Chemicals

Unless specified otherwise, all chemicals were obtained from Sigma-Aldrich.

RESULTS

Localization of different mRNAs encoding NBCe1 variants in adult rat brain

Probe specific to NBCe1-A—We performed *in situ* hybridization using probes to the 5' ORF encoding the unique 41 amino-terminal residues of the A variant (Fig. 1). The antisense A probe displayed very little if any labeling throughout a sagittal section of adult rat brain (Fig. 2A), including the separate olfactory bulb (OB) from a different section. The antisense A probe did not label the cerebellum (Fig. 2B) or hippocampus (Fig. 2C). We performed a positive control by examining hybridization of the antisense probe in rat kidney, where NBCe1-A mRNA and protein are present in the proximal tubule (Romero et al., 1998;Abuladze et al., 1998b;Schmitt et al., 1999;Maunsbach et al., 2000;Aalkjær et al., 2004). The antisense A probe primarily labeled the outer cortex of rat kidney where proximal tubules are present. As seen at higher magnification (Fig. 2D), the probe clearly labeled both proximal tubules (see arrows near the glomerulus (G) in the center of the image) and some distal nephron segments. Therefore, the antisense A probe can detect NBCe1-A mRNA, which appears absent in rat brain.

Probe to NBCe1-B or -C—We next performed *in situ* hybridization using probes to the 5' ORF encoding the different 85 amino-terminal residues of the B and C variants (Fig. 1). In contrast to the absence of antisense A-variant labeling shown in Fig. 2A, we found strong labeling with the antisense B/C probe throughout a sagittal section of adult rat brain (Fig. 2E), but particularly in specific brain regions such as the cerebellum, hippocampus, piriform cortex, as well as olfactory bulb. As a negative control, the sense B/C probe did not exhibit appreciable labeling (Fig. 2F). The punctuate labeling throughout the brain is consistent with NBCe1-B/C

mRNA in astrocytes (Schmitt et al., 2000). In the cerebellum, the antisense-B/C probe labeled both the neuron-rich granule layer and Purkinje layer (Fig. 2G), with labeling in the Purkinje layer consistent with NBCe1-B/C mRNA in Bergmann glia (Fig. 2H). In the hippocampus, the antisense-B/C probe strongly labeled granule neurons in the dentate gyrus (Fig. 2I) and weakly labeled cells in the pyramidal layer (Fig. 2J).

Probe to NBCe1-A/B—According to the data presented in Fig. 2E–J, mRNA encoding the B or C variant is present in brain. To distinguish between these two variants at the mRNA level, we designed probes to the 97-bp sequence found in the 3' ORF of the A and B variants, but not in the C variant (Fig. 1). Because we established that A variant mRNA is nearly absent in brain, this 97-bp probe should primarily detect B-variant mRNA. The antisense A/B probe (Fig. 2K), but not the sense probe (Fig. 2L), exhibited a labeling pattern similar to that seen with the antisense B/C probe, although with lower intensity. One notable exception was labeling of the olfactory bulb by the antisense B/C probe (Fig. 2E) but not the antisense A/B probe (Fig. 2K). The antisense A/B probe labeled the granule and Purkinje layers of the cerebellum (Fig. 2M), and the dentate gyrus and pyramidal layer of the hippocampus (Fig. 2N). The intensity of labeling by the A/B probe was less than that by the B/C probe— a finding consistent with less B than C variant mRNA. However, the different intensities could also reflect different probe lengths. Overall, the data are consistent with the presence of NBCe1-B, and possibly NBCe1-C mRNA in rat brain, with pronounced localization in cerebellum and hippocampus.

Expression of NBCe1 variants in tissue homogenates from different brain regions

To examine the protein expression of NBCe1-B and -C in rat brain, we performed immunoblot analyses using two previously characterized NBCe1 antibodies (Bevensee et al., 2000) that distinguish between the unique 61 carboxy terminal residues of the C variant (αC), and the different 46 residues of the A and B variants (αA/B) (Fig. 1). Because A-variant mRNA appears to be absent or present in low levels in brain (see above), an αA/B signal reflects B-variant expression predominantly. However, we can not definitively exclude NBCe1-A expression if NBCe1-A mRNA in low abundance is undetectable by our probe. In immunoblot studies, we used either 1:500 αA/B (Fig. 3A) or 1:2K αC (Fig. 3B) to probe a commercially available membrane containing protein lysates from 12 different brain regions of adult rat. We also probed the membrane with an antibody to β-actin (αβ-actin, 1:5K), and normalized the intensities of either αA/B or αC to αβ-actin labeling (αA/B:αβ-actin or αC:αβ-actin, respectively).

Both NBC antibodies recognized proteins of the expected size for the NBCe1 variants (~130 kDa), as well as some lower-molecular weight proteins that may be degraded NBCe1 (Schmitt et al., 1999; Bevensee et al., 2000). In addition, faint αC labeling of proteins greater than 199 kDa (Fig. 3B) may represent multimers of NBCe1-C. Among the brain regions, the intensity of αA/B labeling was more variable than that of αC. We obtained similar results on a second commercially available rat-brain membrane. Although there was variability in protein loading per lane based on the αβ-actin labeling, consistent findings in both membranes were relatively high levels of αA/B labeling in the cerebellum and spinal cord (Fig. 3A), and relatively high levels of αC labeling in the hippocampus, medulla, and spinal cord (Fig. 3B). In summary, both NBCe1-B and -C are expressed in many brain regions of adult rat.

Localization of NBCe1 variants in cerebellum, hippocampus, and cortex

Based on our *in situ* hybridization and immunoblot data that are consistent with NBCe1-B and -C expression in rat brain, we next used immunohistochemistry on brain slices from adult rat to explore localization of the proteins in the cerebellum, hippocampus, and cortex. In general, both αA/B and αC exhibited diffuse labeling throughout the brain and in the aforementioned

three regions. In addition, however, each antibody also displayed some distinct labeling as described below.

As described in Methods, we fixed rat brains in Bouin's fixative. Compared to other fixation and antibody labeling protocols that we tested, we found our Bouin's protocol to yield the most consistent labeling patterns with minimum background labeling. However, we obtained similar antibody labeling patterns with αA/B (Supplemental Fig. 1) and αC (Supplemental Fig. 2) using brains from 4% PFA-perfused adult male rats.

NBCe1 expression in cerebellum—αA/B (1:100) only weakly labeled cell layers in the cerebellum. Labeling in the molecular layer was slightly greater than that seen in the granule layer where the nuclei of granule cells are counterstained with blue bis-benzimide (Fig. 4A,B). No labeling was observed in the absence of primary antibody as shown in the negative control image that is merged with the bis-benzimide labeling (-C (Merge), Fig. 4C). αA/B did not appreciably label calbindin-positive Purkinje neurons in the cerebellum (Fig. 4D–F). However, we occasionally observed weak αA/B labeling of some cells in the Purkinje layer of some lobes (not shown).

In contrast, αC (1:500) labeled cells throughout the cerebellum (Fig. 5A,B). No labeling was observed in the absence of primary antibody (Fig. 5C). αC labeling was particularly apparent around the calbindin-positive Purkinje neurons (Fig. 5D–F). The labeling was specific because preabsorbing αC with 100 μg/ml of the corresponding antigenic fusion protein used to generate the antibody (Bevensee et al., 2000) greatly reduced the labeling intensity (Fig. 5G–I). Such competition was not observed with αA/B fusion protein (not shown).

The rim-like labeling of αC is consistent with NBC expression either at the plasma membrane of the Purkinje neurons, or in cell bodies/processes from surrounding glial cells (e.g., Bergmann glia). To explore these possibilities further, we performed co-localization studies with αC and an antibody to the glial cell-specific glutamate transporter GLAST (αGLAST). As shown at both low and higher magnifications (Fig. 5J–O), there was a strong correlation between αC and αGLAST labeling in both the molecular and Purkinje layers of the cerebellum. Both antibodies displayed rim-like labeling around the Purkinje neurons. Thus, the αC labeling in the Purkinje cell layer is likely that of Bergmann glia— data consistent with results from the *in situ* hybridization study (Fig. 2H). On the other hand, we can not exclude the possibility that at least some of the αC labeling in the Purkinje cell layer is neuronal. Indeed, we found some colocalized labeling (not shown) of αC and an antibody to the neuron-localized β1 subunit of the Na^+ pump (Watts et al., 1991; Peng et al., 1997).

NBCe1 expression in hippocampus—Compared to the cerebellar results, αA/B (1:100) weakly labeled cells in the hippocampus, although in a more distinct pattern. More specifically, the antibody labeled cells within all CA pyramidal layers and the dentate gyrus (Fig. 6A–D). As seen at higher magnification of the CA1 layer, αA/B labeled neurons in an intracellular and punctate pattern (Fig. 6E–H). A similar αA/B labeling pattern was seen in other CA layers, as well as the dentate gyrus. As we saw with αC labeling, αA/B labeling was specific because preabsorbing αA/B with 50 μg/ml[1] of the corresponding antigenic fusion protein used to generate the antibody (Bevensee et al., 2000) greatly reduced the labeling intensity (Fig. 6I–L)[2]. αA/B competition was not observed with the αC fusion protein (not shown). The αA/B labeling was clearly neuronal because the cells co-labeled with an antibody to the neuronal

[1]We performed αA/B and αC competition experiments using 20, 50, and 100 μg/ml of the appropriate fusion protein. Overall, the appropriate fusion protein reduced αA/B labeling to a greater extent than αC labeling. αA/B labeling was somewhat reduced by 20 μg/ml and nearly eliminated by 50 and 100 μg/ml fusion protein. However, αC labeling was considerably reduced only at 100 μg/ml fusion protein.

[2]Curiously, there appeared to be more labeling in the cerebellar white matter (not shown) with αA/B and its competitor.

protein MAP2 (Fig. 6M–P), but not with an antibody to the glial protein GFAP (Fig. 6Q–T). In other colocalization studies (not shown), the αA/B-labeled neurons were also labeled with an antibody to the neuronal nuclear protein NeuN.

αC (1:500) also labeled the pyramidal layers and the dentate gyrus of the hippocampus, although the overall labeling was more intense (Fig. 7A–D) than the labeling observed with αA/B. As seen at higher magnification, the αC labeling pattern in the pyramidal layers and dentate gyrus was different than the αA/B labeling pattern. In particular, αC displayed a rim-like labeling pattern around neurons in the pyramidal cell layer (Fig. 7E–H), in contrast to the intracellular, punctate labeling pattern by αA/B (Fig. 6E–H). In the dentate gyrus, αC predominantly labeled cells closer to the center of the hilus (Fig. 7I–K), in contrast to general labeling in the granule cell layer. To evaluate the cell type(s) labeled with αC, we performed colocalization studies with either an antibody to the neuronal protein NeuN or αGLAST. As shown in Fig. 7L–N, NeuN-positive neurons displayed rim-like αC labeling. Based on colocalization studies with αMAP2 (not shown), αC labeling was also evident around the neurons. However, the αC-αNeuN colocalization was moderate, and some of the neurons displayed no or weak αC labeling (see arrows). The colocalization of αGLAST and αC was much stronger in both the pyramidal layers (Fig. 7O–Q) and the dentate gyrus (Fig. 7R–T). The data are consistent with αC labeling of glial cells predominantly in the pyramidal layers and dentate gyrus of the hippocampus. Similar hippocampal results were obtained with triple labeling with αC, αMAP2, and αGLAST.

NBCe1 expression in cortex—Similar to that seen in the hippocampus, αA/B (1:100) exhibited punctate, intracellular labeling in the cortex (Fig. 8A,D). The labeled cells appeared to be neurons because a majority of them co-labeled with the antibody to the neuronal protein MAP2 (Fig. 8B, C, see arrows). In contrast, αC (1:500) labeling was more diffuse and more apparent around neuronal cell bodies (Fig. 8E,H,I,L) that were NeuN-positive (Fig. 8F,G). The labeling was more glial than neuronal because of strong co-localization with the glial marker GLAST (Fig. 8J,K).

High-resolution NBCe1 expression in cerebellum—Immunoelectron microscopy showed the subcellular localization of αC and αA/B in the Purkinje layer of cerebellum. Colloidal gold particles representing αC labeling were preferentially associated with the plasma membrane of glial cells (Fig. 9A,B), identified through their shape or occasional apposition to the outer surface of capillaries. Although αC primarily labeled the plasma membrane of glial cells, we can not exclude the possibility that αC may have also labeled the plasma membrane of neurons in some instances. However, αC labeling followed the very complex periphery of the glial cells and included long stretches of membrane. Numerous small nerve processes nearby did not express αC. Occasional gold particles close to the periphery of some thicker nerve fiber appeared related to adjacent glial cells. αA/B on the contrary was expressed in the cytoplasm of some nerve cell fibers (Fig. 9C), but many large and all small fibers were unlabeled. Gold particles in the labeled fibers were often in filamentous areas in the cytoplasm and occasionally in the endoplasmic reticulum (ER).

DISCUSSION

In the present study, we examined the localization and expression of the three NBCe1 variants (A, B, and C) in rat brain. According to *in situ* hybridization data, A variant mRNA appears to be absent, whereas B and possibly C variant mRNA is present throughout brain, particularly in the cerebellum and hippocampus. However, we can not exclude the possibility that A-variant mRNA is present at a very low level, which may be difficult to detect with our short probe that is unavoidably near the detection threshold. In an important control experiment however, the A probe does detect NBC mRNA in kidney. In support of our *in situ* hybridization results, we

and others (MF Romero, *personal communication*) have had difficulty amplifying NBCe1-A cDNA from rat brain.

Based on the near absence or low level of A-variant mRNA in brain, αNBCe1-A/B labeling in our immunohistochemistry studies reflects B variant expression predominantly. αA/B clearly labeled neurons, whereas αC appeared to label glial cells more so than neurons in the hippocampus and cortex. Furthermore, αA/B labeling was intracellular and punctate compared to αC labeling that surrounded neurons. Intracellular expression of NBCe1-B in neurons and plasma-membrane expression of NBCe1-C in glial cells was supported by immunogold electron microscopy data obtained from the cerebellum.

An intriguing observation was the intracellular localization profile of NBCe1 in neurons. According to the electron microscopy data (Fig. 9C), αA/B labeled cytoplasmic regions containing filamentous structures, and in some cases, the ER. Although it is not clear if the filaments and ER are labeled, the transporter may be in transit by itself or as some complex. While the functional role of a cytoplasmic NBC is unknown, an NBC in the membrane of an organelle such as the ER may play a role in organellar pH regulation similar to that seen with NHE6-9 (Nakamura et al., 2005). On the other hand, it is somewhat surprising if NBCe1 is targeted to a cytoplasmic compartment in neurons because NBCe1-A/B is targeted to basolateral membranes of other cells types, including the kidney proximal tubule and the pancreatic ducts (Romero et al., 2004). Alternatively, the plasma membrane may be the target site in neurons, and NBCe1 expression is normally low and/or requires a stimulus for increased surface expression. It is important to point out that the level or mode of NBCe1 activity may be different for the transporter in the cytoplasm vs. plasma membrane. For instance, polycystin-2 (PKD2) functions as an intracellular Ca^{2+}-release channel in the ER, where it predominantly resides, but as a receptor-operated nonselective cation channel in the plasma membrane (Tsiokas et al., 2007).

In comparing results from the *in situ* hybridization and immunohistochemistry data, the similarities exceed the differences. The similarities support the expression of both NBCe1-B and NBCe1-C in brain. For example, the major brain regions (e.g., cerebellum and hippocampus) labeled with the mRNA probes were also labeled with the two antibodies. In fact, each region labeled with the B/C probe was also labeled with one or both of the antibodies. For example, labeling of Bergmann glia in the cerebellum by the B/C probe (Fig. 2H) is consistent with αC labeling around the Purkinje neurons (Fig. 5D) that co-localizes with αGLAST labeling (Fig. 5M). Labeling of hippocampal cells in the dentate gyrus by the B/C mRNA probe (Fig. 2I) —and to a lesser extent the CA layers (Fig. 2J)— is consistent with αA/B (Fig. 6) and/or αC labeling (Fig. 7). In all likelihood, B/C probe-positive cells in the internal portion of the dentate gyrus hilus are glial precursor cells based on the pattern of αC labeling and co-localization with the glial marker GLAST (Fig. 7I–K,R–T). For the A/B probe (which detects NBCe1-B primarily in brain), labeling in the dentate gyrus and CA layers was also evident (Fig. 2K,N) and consistent with αA/B labeling (Fig. 6).

Regarding differences between the mRNA and protein localization data, both the B/C and A/B probes weakly label the pyramidal layer compared to the dentate gyrus (Fig. 2I,J,N), whereas both antibodies show pronounced labeling (Fig. 6A and Fig. 7A). Also, both probes labeled the granule layer of the cerebellum more so than the molecular layer (Fig. 2E,H,K,M), whereas the two antibodies labeled the two layers to the same extent or the molecular layer to a greater extent (Fig. 4 and Fig. 5). Mismatches between mRNA and protein levels are not uncommon, and may be due to differences in translation efficiency, protein turnover, etc.

It is important to point out that there appears to be differences in NBC localization *in situ* vs. *in vitro*. For example, according to immunoblot data on microsomal protein from cultured

cortical cells, the A/B variant is predominant in astrocytes vs. neurons, and the opposite is true for the C variant (Bevensee et al., 2000). We have more recently obtained similar results on cultured hippocampal cells (Majumdar, Williams, Bevensee; unpublished data). Thus, NBC expression profiles are different for cells in culture.

Electrogenic NBC activity has been identified and characterized in mammalian astrocytes *in situ* (Grichtchenko and Chesler, 1994a; Grichtchenko and Chesler, 1994b), as well as cultured from several brain regions (Bevensee et al., 1997a; Bevensee et al., 1997b; O'Connor et al., 1994; Brune et al., 1994). Our data are consistent with NBCe1-C being responsible for such activity *in situ*, although NBCe1-B activity may play a larger role when astrocytes are cultured. To date, electrogenic NBC activity has not been reported in neurons, although we have recently found a population of cultured hippocampal neurons that exhibit such activity (Majumdar, Wu, McNicholas-Bevensee, Bevensee, unpublished data). Based on our *in situ* hybridization and immunochemistry data, as well as the aforementioned immunoblot data, it would not be surprising to find NBCe1 expression at the plasma membrane of cultured neurons.

As described in the Introduction, results from early molecular and localization studies stemming from the cloning of NBCs are consistent with the expression of NBCe1 variants in brain. Both NBCe1-B and NBCe1-C –but not NBCe1-A– were cloned by homology from a rat-brain cDNA library (Bevensee et al., 2000). Using polynucleotide probes and/or polyclonal antibodies that did not distinguish among the three NBCe1 variants, Schmitt et al. (Schmitt et al., 2000) and Giffard et al. (Giffard et al., 2000) found NBCe1 widely distributed throughout the rat brain —especially the cerebellum and hippocampus— and localized to glial cells and some neurons. In addition, Giffard et al. (Giffard et al., 2000) found minimal expression of A variant mRNA. Our results complement and extend these findings. For example, we also found minimal expression of A-variant mRNA in our *in situ* hybridization studies, but pronounced B- and/or C-variant mRNA expression throughout the brain, particularly in the cerebellum and hippocampus. At the protein level, neurons were labeled with αA/B, whereas glial cells were primarily labeled with αC.

More recently, Rickmann et al. (Rickmann et al., 2007) reported on the expression profiles of the A and B variants in adult mouse brain using N-terminal antibodies. In contrast to our findings, as well as those of Giffard et al. (Giffard et al., 2000) working on rat, Rickmann et al. (Rickmann et al., 2007) described the localization of NBCe1-A mRNA in several brain regions (e.g., olfactory bulb, cerebral cortex, hippocampus, and cerebellum) and expression of the protein in neuronal populations/regions including *i*) Purkinje cell bodies and dendrites of the cerebellum, *ii*) granule cells, non-pyramidal neurons, and apical cell dendrites in the hippocampus, and *iii*) pyramidal neurons (and some astroglial lamellae) in the cerebral cortex. The discrepancy between our A-variant data and those of the Rickmann group is not clear, although a species difference may be responsible.

Rickmann et al. (Rickmann et al., 2007) also reported that NBCe1-B mRNA is present in the same brain regions as described above for NBCe1-A. However, the profile of protein expression is different. For example, the group's NBCe1-B antibody labeled *i*) Bergmann glia and Purkinje cell bodies (weakly) of the cerebellum, *ii*) non-pyramidal neurons, apical cell dendrites, and perivascular astroglial compartments in the hippocampus, and *iii*) pyramidal neurons (weakly) and astroglial processes (weakly) in the cerebral cortex. However, because this NBCe1-B antibody is also expected to recognize the C variant as well, the labeling patterns likely reflect B and/or C variant expression. Therefore, it is not surprising that one or both of our NBCe1 antibodies recognize most of these regions. Consistent with our findings, the authors reported localization of NBCe1-B in the rough endoplasmic reticulum of cerebellar neurons.

As described in the Introduction, electrogenic NBC activity has been extensively studied in astrocytes, where the transporter can modulate neuronal activity through changes in pH_i/pH_o. However, the functional significance of electrogenic NBC activity in neurons is poorly understood. It is well known that neurons exhibit a decrease in pH_i upon firing (in some preparations due to Ca^{2+}-pump mediated exchange of intracellular Ca^{2+} and extracellular H^+ following an elevation of intracellular Ca^{2+}) (McAlear and Bevensee, 2003; Chesler, 2003). The firing-evoked pH_i decrease would be expected to stimulate the activity of an electrogenic NBC in neurons, thereby reducing the magnitude of the pH_i decrease. Neuronal depolarization would also stimulate electrogenic NBC activity, and further retard the pH_i decrease.

An obvious question pertains to the importance of multiple NBCe1 variants in brain. Although the physiological significance of the three NBCe1 variants with different amino and/or carboxy termini is not fully known, these regions may influence expression at the plasma membrane or regulation by signaling molecules or binding proteins. One of the distinguishing features of the C variant compared to the A and B variants is a PDZ-binding motif at the carboxy terminus (Bevensee et al., 2000). This motif may confer C variant-specific regulation by PDZ proteins in certain cells.

Changes in NBCe1 expression have been associated with development and disease, although little is known about the involvement of specific variants. For example, general NBCe1 expression in rat brain increases progressively from embryonic d 16 until postnatal d 105, particularly in the brainstem-diencephalon and cerebellum compared to the cortex (Douglas et al., 2001). NBCe1 expression has also been correlated to neuropathologies such as epilepsy. For example, general NBCe1 immunoreactivity is elevated in the hippocampus of the gerbil from 30 min to 3 h after the onset of seizure, but then returns to the pre-seizure level at 6 h (Kang et al., 2002). In light of the results herein, further studies are required to assess the influence of different NBCe1 variants on pH_i regulation during development or diseases such as epilepsy.

In conclusion, we have examined mRNA localization and protein expression of the three NBCe1 variants in rat brain. According to our studies, NBCe1-B and NBCe1-C, but not NBCe1-A are the predominant NBCe1 variants expressed in brain, particularly in the cerebellum, hippocampus, and cortex. In the hippocampus and cortex, NBCe1-B is localized intracellularly in neurons. NBCe1-C is expressed primarily in glia surrounding neurons and possibly neurons within the neuropil of the pyramidal cell and granule layers of the hippocampus, the Purkinje cell layer of the cerebellum, and the cortex. The general role of NBCs in the brain is to regulate pH_i and pH_o. Distinct expression profiles of NBCe1 variants may contribute to specific pH physiologies seen with development or disease state.

Supplementary Material

Refer to Web version on PubMed Central for supplementary material.

LIST OF ABBREVIATIONS

BSA, bovine serum albumin
BT, bicarbonate transporter
DIG, digoxigenin
ER, endoplasmic reticulum
HRP, horseradish peroxidase
K^+_o, extracellular K^+
MAP2, microtubule-associated protein
MBP, maltose binding protein

NBCe1 (or 2), electrogenic Na/bicarbonate cotransporter 1 (or 2)
NBCn1, electroneutral Na/bicarbonate cotransporter 1
NDCBE, Na-driven Cl-bicarbonate exchanger
NeuN, neuronal nuclei
OB, olfactory bulb
ORF, open reading frame
PBS, phosphate-buffered saline
PFA, paraformaldehyde
pH_i, intracellular pH
pH_o, extracellular pH
RT, room temperature

ACKNOWLEDGMENTS

This work was supported by NIH/NINDS NS046653 (M.O.B), AHA predoctoral fellowship 0415264B (D.M.), and the UAB Neuroscience Core Facilities NS 47466. This work was supported by NIH Neuroscience Blueprint Core Grant NS57098 to the University of Alabama at Birmingham. We thank Cecelia B. Latham for her expertise in immunohistochemistry, Albert Tousson for assistance with the confocal microscopy at the high resolution imaging facility at UAB, Dr. Lori L. McMahon for evaluating our immunolabeling and providing valuable suggestions, Dr. Michael J. Caplan (Yale University) for providing thoughtful comments regarding our electron microscopy data, Dr. Peter R. Smith and his laboratory for use of his fluorescence microscope, Dr. Buffie Clodfelder-Miller for taking pictures of the *in situ* labeling, Dr. Jim Schafer for evaluating our *in situ* hybridization data from kidney, the laboratory of Dr. John J. Hablitz for providing the GLAST antibody, the laboratory of Dr. David F. Crawford for providing the β-actin antibody, and laboratory of Dr. Marcas Bamman for help with the densitometry analysis, and Dr. Carmel M. McNicholas-Bevensee for valuable comments regarding the manuscript.

REFERENCES

Aalkjær C, Frische S, Leipziger J, Nielsen S, Praetorius J. Sodium coupled bicarbonate transporters in the kidney, an update. Acta Physiol Scand 2004;181:505–512. [PubMed: 15283764]

Abuladze N, Lee I, Newman D, Hwang J, Boorer K, Pushkin A, Kurtz I. Molecular cloning, chromosomal localization, tissue distribution, and functional expression of the human pancreatic sodium bicarbonate cotransporter. J Biol Chem 1998a;273:17689–17695. [PubMed: 9651366]

Abuladze N, Lee I, Newman D, Hwang J, Pushkin A, Kurtz I. Axial heterogeneity of sodium-bicarbonate cotransporter expression in the rabbit proximal tubule. Am J Physiol 1998b;274:F628–F633. [PubMed: 9530281]

Berger UV, Hediger MA. Differential distribution of the glutamate transporters GLT-1 and GLAST in tanycytes of the third ventricle. J Comp Neurol 2001;433:101–114. [PubMed: 11283952]

Bevensee MO, Apkon M, Boron WF. Intracellular pH regulation in cultured astrocytes from rat hippocampus. II. Electrogenic Na/HCO_3 cotransport. J Gen Physiol 1997a;110:467–483. [PubMed: 9379176]

Bevensee MO, Schmitt BM, Choi I, Romero MF, Boron WF. An electrogenic Na/HCO_3 cotransporter (NBC) with a novel C terminus, cloned from rat brain. Am J Physiol Cell Physiol 2000;278:C1200–C1211. [PubMed: 10837348]

Bevensee MO, Weed RA, Boron WF. Intracellular pH regulation in cultured astrocytes from rat hippocampus. I. Role of HCO_3^-. J Gen Physiol 1997b;110:453–465. [PubMed: 9379175]

Brune T, Fetzer S, Backus KH, Deitmer JW. Evidence for electrogenic sodium-bicarbonate cotransport in cultured rat cerebellar astrocytes. Pflügers Arch 1994;429:64–71.

Burnham CE, Amlal H, Wang Z, Shull GE, Soleimani M. Cloning and functional expression of a human kidney $Na^+:HCO_3^-$ cotransporter. J Biol Chem 1997;272:19111–19114. [PubMed: 9235899]

Chesler M. The regulation and modulation of pH in the nervous system. Prog Neurobiol 1990;34:401–427. [PubMed: 2192394]

Chesler M. Regulation and modulation of pH in the brain. Physiol Rev 2003;83:1183–1221. [PubMed: 14506304]

Chesler M, Kaila K. Modulation of pH by neuronal activity. Trends Neurosci 1992;15:396–402. [PubMed: 1279865]

Choi I, Romero MF, Khandoudi N, Bril A, Boron WF. Cloning and characterization of a human electrogenic Na^+-HCO_3^- cotransporter isoform (hhNBC). Am J Physiol 1999;276:C576–C584. [PubMed: 10069984]

Deitmer JW. Evidence for glial control of extracellular pH in the leech central nervous sytem. Glia 1992;5:43–47. [PubMed: 1531809]

Deitmer JW, Schlue W-R. The regulation of intracellular pH by identified glial cells and neurones in the central nervous system of the leech. J Physiol (Lond) 1987;388:261–283. [PubMed: 2821243]

Deitmer JW, Schlue W-R. An inwardly directed electrogenic sodium-bicarbonate cotransport in leech glial cells. J Physiol (Lond) 1989;411:179–194. [PubMed: 2559193]

Douglas RM, Schmitt BM, Xia Y, Bevensee MO, Biemesderfer D, Boron WF, Haddad GG. Sodium-hydrogen exchangers and sodium-bicarbonate co-transporters: ontogeny of protein expression in the rat brain. Neuroscience 2001;102:217–228. [PubMed: 11226686]

Giffard RG, Papadopoulos MC, van Hooft JA, Xu L, Giuffrida R, Monyer H. The electrogenic sodium bicarbonate cotransporter: developmental expression in rat brain and possible role in acid vulnerability. J Neurosci 2000;20:1001–1008. [PubMed: 10648705]

Grichtchenko II, Chesler M. Depolarization-induced acid secretion in gliotic hippocampal slices. Neuroscience 1994a;62:1057–1070. [PubMed: 7845586]

Grichtchenko II, Chesler M. Depolarization-induced alkalinization of astrocytes in gliotic hippocampal slices. Neuroscience 1994b;62:1071–1078. [PubMed: 7845587]

Kang TC, An SJ, Park SK, Hwang IK, Suh JG, Oh YS, Bae JC, Won MH. Alterations in Na^+/H^+ exchanger and Na^+/HCO_3^- cotransporter immunoreactivities within the gerbil hippocampus following seizure. Brain Res Mol Brain Res 2002;109:226–232. [PubMed: 12531533]

Katsura, K.; Siesjo, B. Acid-base metabolism in ischemia. In: Kaila, K.; Ransom, B., editors. pH and Brain Function. New York: Wiley-Liss, Inc.; 1998. p. 563-582.

Majumdar D, Shacka JJ, Williams JB, Berger UV, Schultz K, Harkins LE, Roth KA, Bevensee MO. Localization of electrogenic Na/bicarbonate cotransporter NBCe1 variants in rat brain. Soc.Neurosci.Abst 2006;33#729.2

Maunsbach AB, Vorum H, Kwon TH, Nielsen S, Simonsen B, Choi I, Schmitt BM, Boron WF, Aalkjær C. Immunoelectron microscopic localization of the electrogenic Na/HCO_3 cotransporter in rat and *Ambystoma* kidney. J Am Soc Nephrol 2000;11:2179–2189. [PubMed: 11095641]

McAlear, SD.; Bevensee, MO. pH regulation in non-neuronal brain cells and interstitial fluid. In: Hertz, L., editor. Non-neuronal cells of the nervous system: Function and dysfunction. Amsterdam: Elsevier; 2003. p. 707-745.

Nakamura N, Tanaka S, Teko Y, Mitsui K, Kanazawa H. Four Na^+/H^+ exchanger isoforms are distributed to Golgi and post-Golgi compartments and are involved in organelle pH regulation. J Biol Chem 2005;280:1561–1572. [PubMed: 15522866]

O'Connor ER, Sontheimer H, Ransom BR. Rat hippocampal astrocytes exhibit electrogenic sodium-bicarbonate cotransport. J Neurophysiol 1994;72:2580–2589. [PubMed: 7897475]

Peng L, Martin-Vasallo P, Sweadner KJ. Isoforms of Na, K - ATPase α and β subunits in the rat cerebellum and in granule cell cultures. J Neurosci 1997;17:3488–3502. [PubMed: 9133374]

Ransom BR. Glial modulation of neural excitability mediated by extracellular pH: A hypothesis. Prog Brain Res 1992;94:37–46. [PubMed: 1287724]

Ransom BR. Glial modulation of neural excitability mediated by extracellular pH: a hypothesis revisited. Prog Brain Res 2000;125:217–228. [PubMed: 11098659]

Rickmann M, Orlowski B, Heupel K, Roussa E. Distinct expression and subcellular localization patterns of Na^+/HCO_3^- cotransporter (SLC 4A4) variants NBCe1-A and NBCe1-B in mouse brain. Neuroscience 2007;146:1220–1231. [PubMed: 17433553]

Romero MF, Fong P, Berger UV, Hediger MA, Boron WF. Cloning and functional expression of rNBC, an electrogenic Na^+-HCO_3^- cotransporter from rat kidney. Am J Physiol 1998;274:F425–F432. [PubMed: 9486238]

Romero MF, Fulton CM, Boron WF. The SLC4 family of HCO_3^- transporters. Pflügers Arch 2004;447:495–509.

Romero MF, Hediger MA, Boulpaep EL, Boron WF. Expression cloning and characterization of a renal electrogenic Na^+/HCO_3^- cotransporter. Nature 1997;387:409–413. [PubMed: 9163427]

Rose, CR.; Ransom, BR. pH regulation in mammalian glia. In: Kaila, K.; Ransom, B., editors. pH and Brain Function. New York: Wiley-Liss, Inc.; 1998. p. 253-275.

Schmitt BM, Berger UV, Douglas RM, Bevensee MO, Hediger MA, Haddad GG, Boron WF. Na/HCO_3 cotransporters in rat brain: expression in glia, neurons, and choroid plexus. J Neurosci 2000;20:6839–6848. [PubMed: 10995828]

Schmitt BM, Biemesderfer D, Romero MF, Boulpaep EL, Boron WF. Immunolocalization of the electrogenic Na^+/HCO_3^- cotransporter in mammalian and amphibian kidney. Am J Physiol 1999;276:F27–F36. [PubMed: 9887077]

Tsiokas L, Kim S, Ong EC. Cell biology of polycystin-2. Cell Signal 2007;19:444–453. [PubMed: 17084592]

Watts AG, Sanchez-Watts G, Emanuel JR, Levenson R. Cell-specific expression of mRNAs encoding Na^+, K^+, - ATPase α- and β- subunit isoforms within the rat central nervous system. Proc Natl Acad Sci USA 1991;88:7425–7429. [PubMed: 1651505]

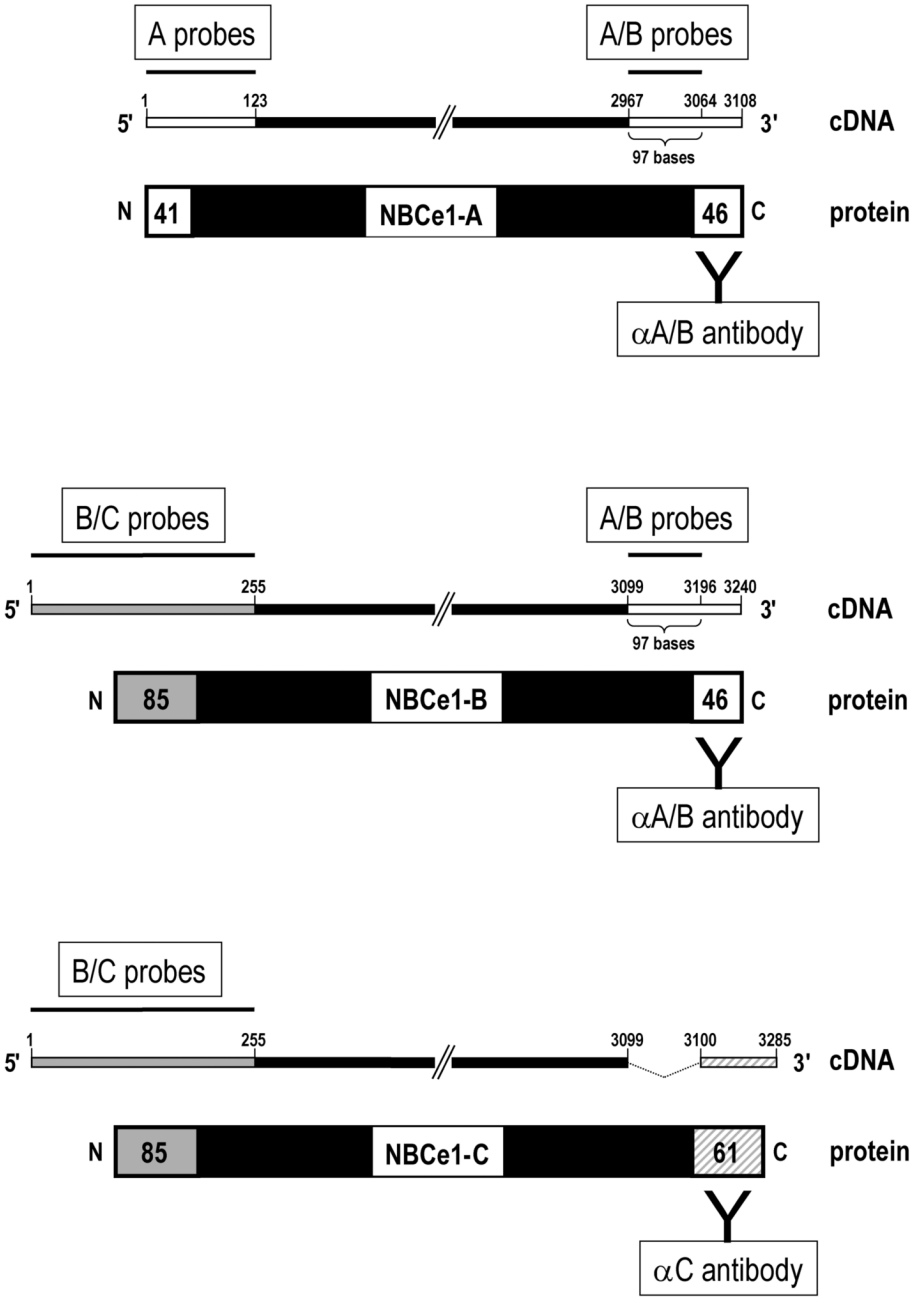

Fig. 1.

In situ hybridization probes and rabbit polyclonal antibodies for localizing NBCe1-A, -B, and -C variants in rat brain. The cDNA and protein diagrams are not drawn to scale. Antisense and sense A probes recognize the unique 5' ORF (bp 1–123) that encodes the unique amino-terminal 41 residues of the A variant. Antisense and sense B/C probes recognize the different 5' ORF (bp 1–255) that encodes the different amino-terminal 85 residues of the B and C variants. Antisense and sense A/B probes recognize the 97-bp region near the 3' end of the ORF found in the A and B variants, but not the C variant. Two different rabbit polyclonal antibodies previously characterized (Bevensee et al., 2000) distinguish between the C-terminal 46 residues

of the A and B variants (αA/B antibody) and the unique C-terminal 61 residues of the C variant (αC antibody).

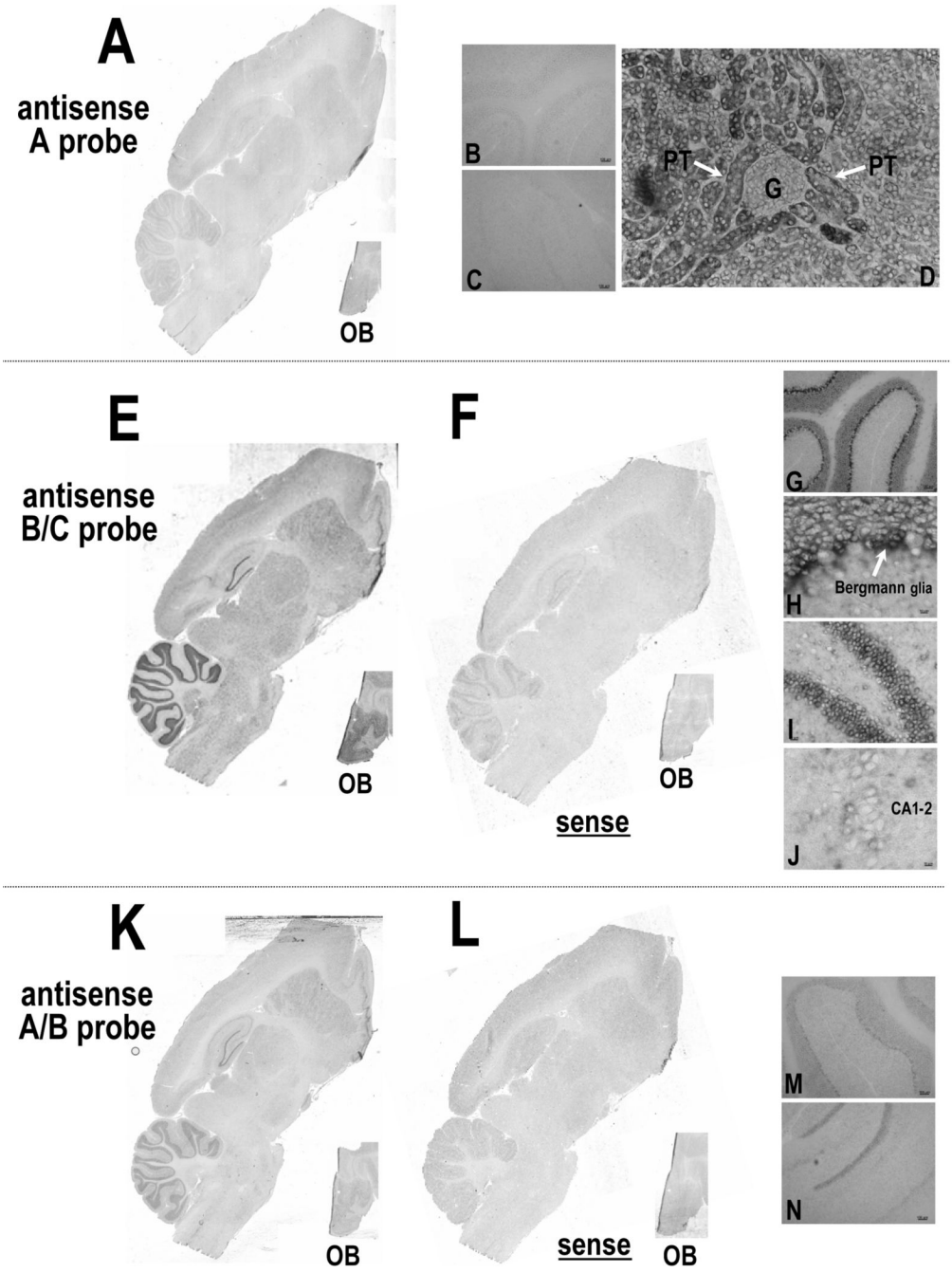

Fig. 2.

Localization of mRNA encoding NBCe1 variants in rat brain. (A–D) A specific antisense probe to the 5' ORF of NBCe1-A. Little NBCe1-A mRNA was detected throughout brain (A), including the cerebellum (B) and the hippocampus (C). As a positive control, the antisense probe labeled the outer cortex and proximal tubules near the glomerulus (G) of rat kidney (D). (E–J) A specific antisense probe to the 5' ORF of NBCe1-B/C variants. NBCe1-B/C mRNA was present throughout brain, particularly in the cerebellum and hippocampus, as well as the olfactory bulb (OB) shown in the inset (E). Minimal labeling was obtained with the sense probe (F). NBCe1-B/C mRNA was prominent in (*i*) the granular and Purkinje layers of the cerebellum (G, H), especially Bergmann glia in the Purkinje layer (H), and (*ii*) the dentate gyrus of the

hippocampus (I). NBCe1-B/C mRNA was less pronounced in the pyramidal layer of the hippocampus (J). (K–N) A specific antisense probe to the 3' ORF of NBCe1-A/B variants. NBCe1-A/B mRNA was present throughout brain (K), as well as cerebellum (M) and hippocampus (N), in a pattern similar to that seen with the B/C antisense probe. Minimal labeling was obtained with the sense probe (L). Numbers above scale bars in panels are in micrometers.

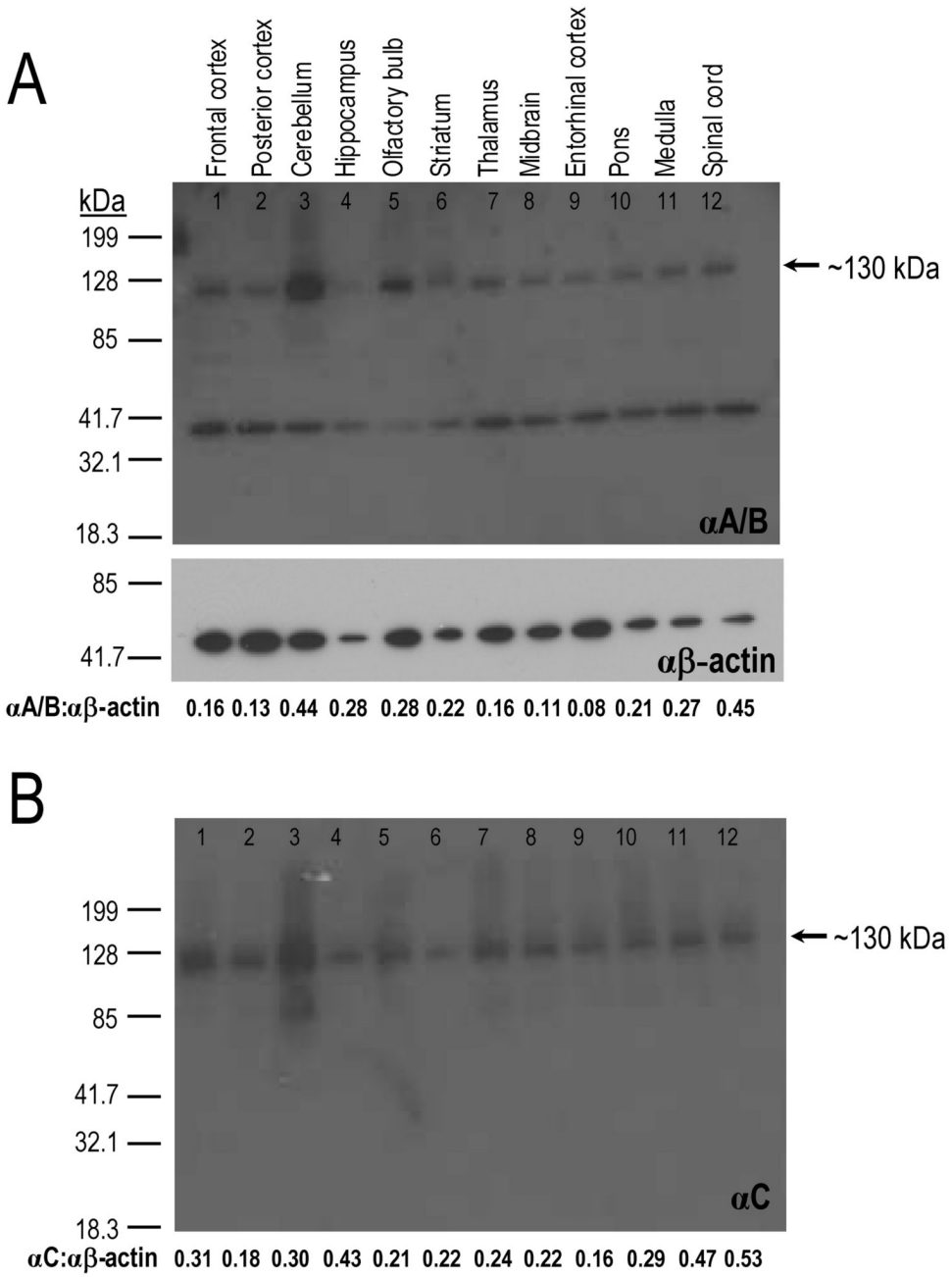

Fig. 3.

Expression of NBCe1 variants in tissue homogenates from different regions of rat brain. (A, top) A commercially available blot containing total protein from various brain regions probed with 1:500 αA/B. NBCe1-A/B is ~130 kDa. (A, bottom) The same commercial blot was reprobed with 1:5000 αβ-actin. Intensity of αA/B labeling normalized to that of αβ-actin is shown as αA/B:αβ-actin. (B) The blot probed with 1:2000 αC. NBCe1-C is ~130 kDa. Intensity of αC labeling normalized to that of αβ-actin is shown as αC:αβ-actin.

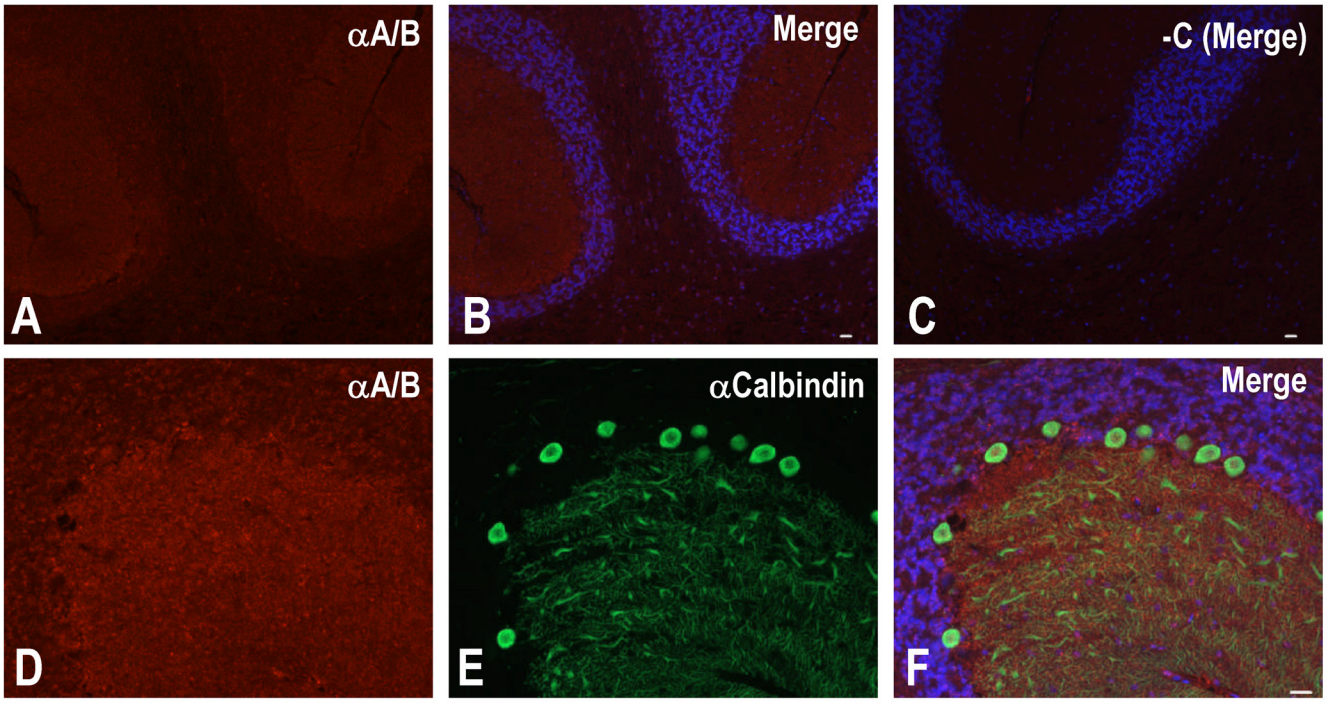

Fig. 4.

NBCe1-A/B expression in rat cerebellum. (A–C) Fluorescence microscopy image of weak αA/B labeling in the cerebellum of a sagittal brain section. αA/B labeling of the molecular layer was slightly greater than the granule layer (A). Images of αA/B labeling and nuclear bis benzimide staining are overlaid (B). No labeling was seen in the negative control without primary antibody (C). Scale bar = 20 μm for A–C. (D–F) Fluorescence microscopy image of double labeling by αA/B (D) and αCalbindin (1:1K) (E) in the cerebellum of a sagittal brain section. There was minimal colocalization seen in the merged figure (F). Scale bar = 20 μm for D–F.

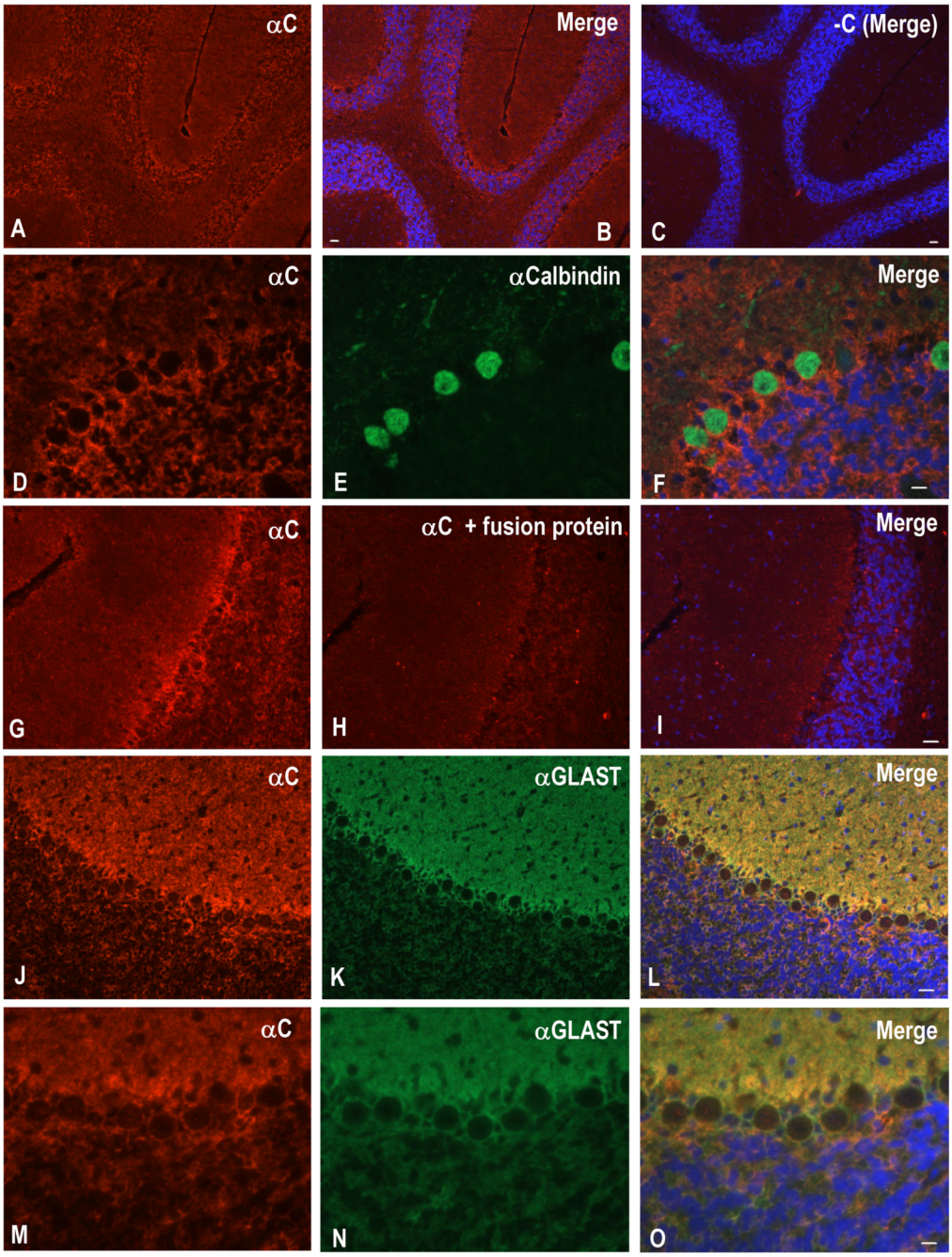

Fig. 5.

NBCe1-C expression in rat cerebellum. (A–C) Fluorescence microscopy image of αC labeling in the cerebellum of a sagittal brain section. αC labeled the granule and the Purkinje cell layers (A). Images of αC labeling and nuclear bis benzimide staining are overlaid (B). No labeling was seen in the negative control without primary antibody (C). Scale bar = 20 μm for A–C. (D–F) Fluorescence microscopy image of double labeling of αC and αCalbindin (1:1K) in the cerebellum of a sagittal brain section. Colocalization of αC (D) and αCalbindin (E) was consistent with NBCe1-C expression around the Purkinje neurons as seen in the merged image (F). Scale bar = 10 μm for D–F. (G–I) Fluorescence microscopy image showing the specificity of αC labeling in the cerebellum of a sagittal brain section. αC labeling (G) was reduced by

preabsorption with 100 μg/ml fusion protein (H,I). Scale bar = 20 μm for G–I. (J–O) Fluorescence microscopy images of double labeling by αC and αGLAST (1:500) at lower (J–L) and higher (M–O) magnifications in the cerebellum of a sagittal brain section. Colocalization of αC (J,M) and αGLAST (K,N) was consistent with NBCe1-C expression in glia within the Purkinje cell layer as seen in the merged image (L, O). Scale bars = 20 μm for J–L, and 10 μm for M–O.

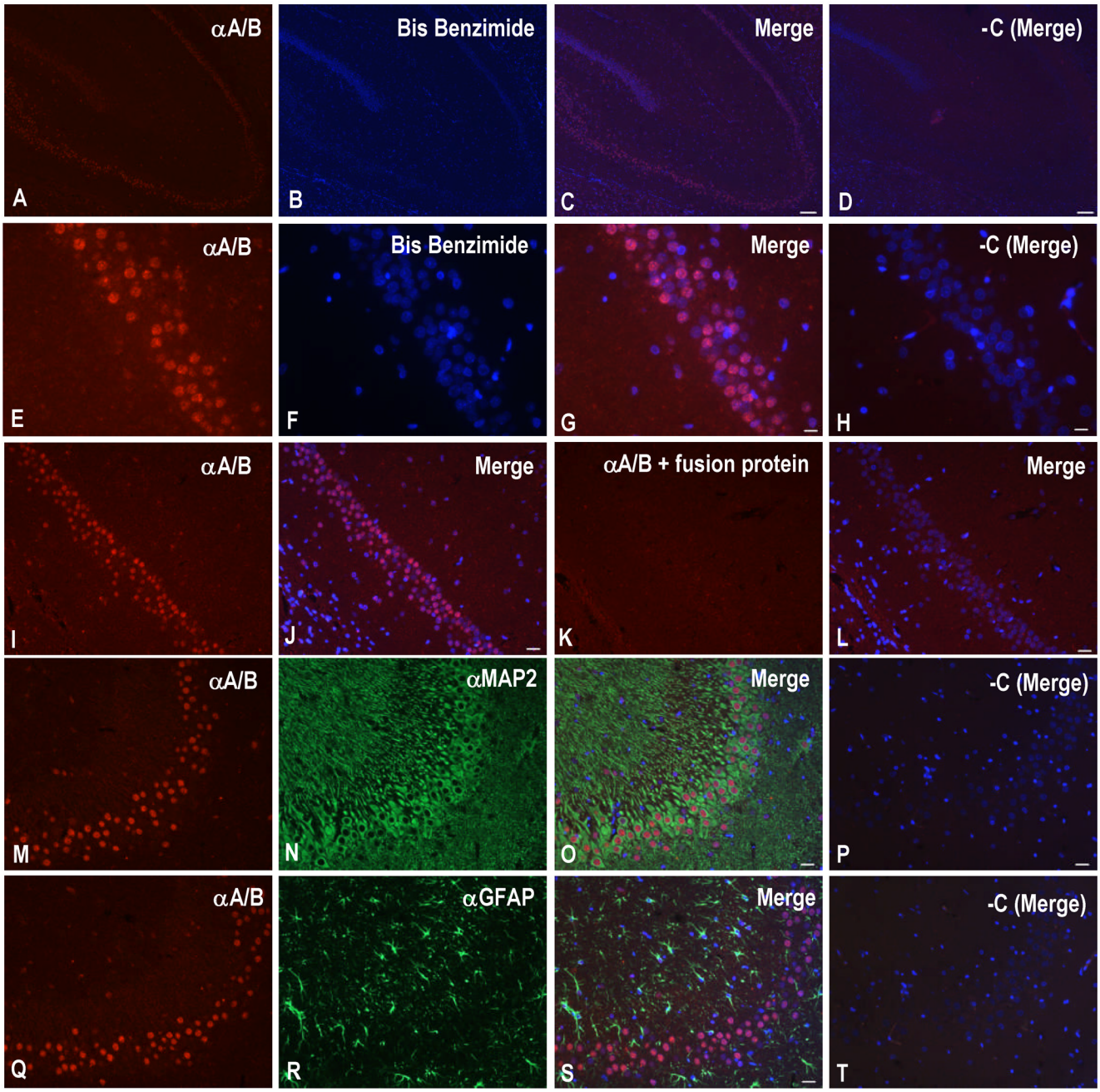

Fig. 6.

NBCe1-A/B expression in rat hippocampus. (A–D) Fluorescence microscopy image of intracellular αA/B labeling in the hippocampus of a sagittal brain section. αA/B (A) exhibited punctate intracellular labeling in the pyramidal cell layer and the dentate gyrus of the hippocampus. Images of αA/B labeling (A) and nuclear bis benzimide staining (B) are overlaid (C). No labeling was seen in the negative control without primary antibody (D). Scale bar = 100 μm for A–D. (E–H) Fluorescence microscopy image of intracellular αA/B labeling in the CA1 layer of a sagittal brain section. Images of αA/B labeling (E) and nuclear bis benzimide staining (F) are overlaid (G). No labeling was seen in the negative control without primary antibody (H). Scale bar = 10 μm for E–H. (I–L) Fluorescence microscopy image showing the

specificity of αA/B labeling in the CA1 layer of a sagittal brain section. αA/B labeling (I,J) was reduced by preabsorption with 50 μg/ml fusion protein (K,L). Scale bar = 20 μm for I–L. (M–P) Fluorescence microscopy image of intracellular αA/B labeling in the CA3a layer of a sagittal brain section. Colocalization of αA/B (M) and αMAP2 (1:100K) (N) was consistent with NBCe1-A/B expression in the pyramidal cells as seen in the merged image (O). No labeling was seen in the negative control without primary antibody (P). Scale bar = 20 μm for M–P. (Q–T) Fluorescence microscopy image of distinct αA/B and αGFAP (1:5K) labeling in the CA3a layer of sagittal brain section. αA/B (Q) and αGFAP (R) did not colocalize– a finding consistent with the absence of NBCe1-A/B in astrocytes as seen in the merged image (S). No labeling was seen in the negative control without primary antibody (T). Scale bar = 20 μm for Q–T.

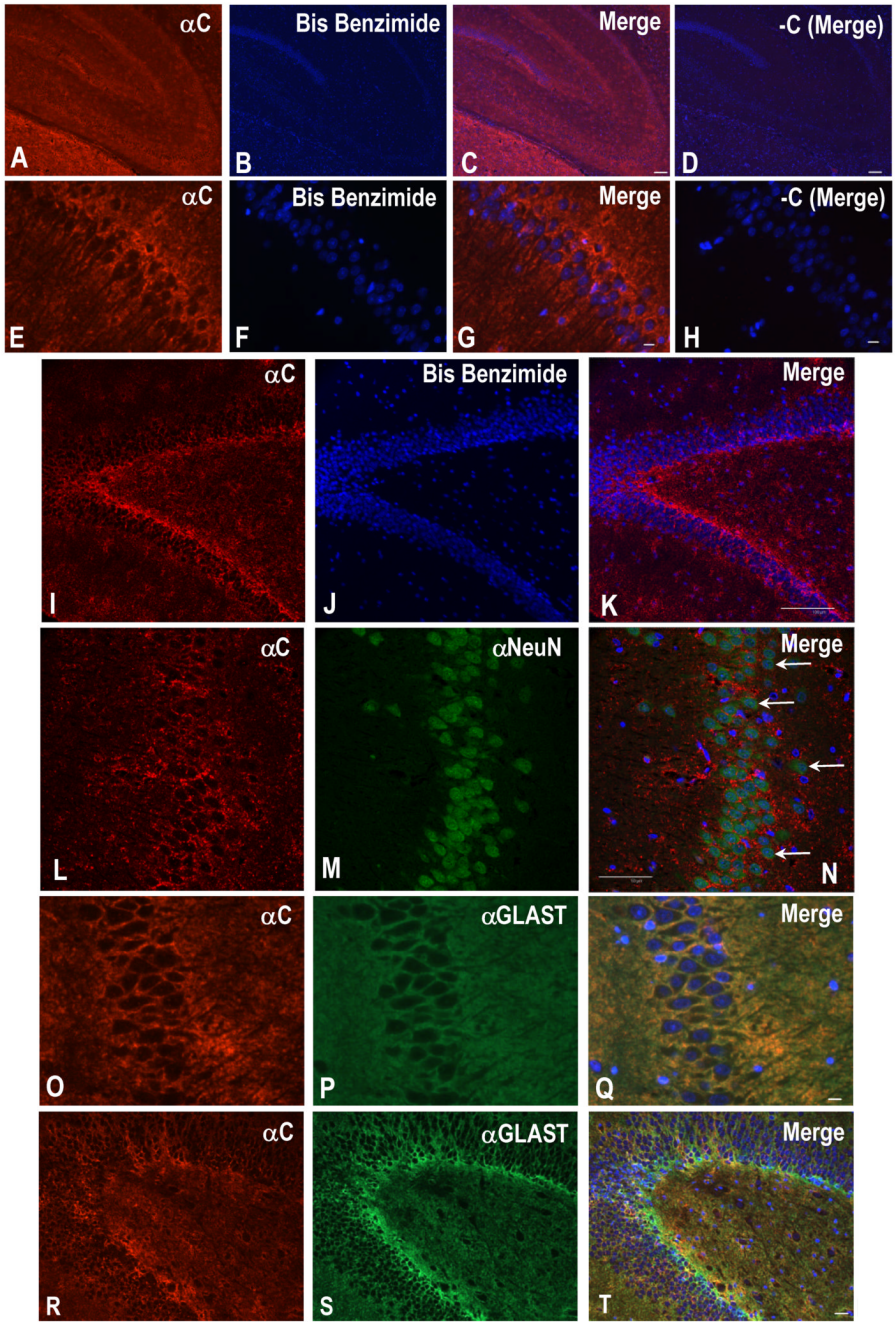

Fig. 7.

NBCe1-C expression in rat hippocampus. (A–D) Fluorescence microscopy image of αC labeling in the hippocampus of a sagittal brain section. αC (A) labeled the pyramidal cell layer and dentate gyrus. Images of αC labeling (A) and nuclear bis benzimide staining (B) are overlaid (C). No labeling was seen in the negative control without primary antibody (D). Scale bar = 100 μm for A–D. (E–H) Fluorescence microscopy image of rim-like αC labeling in the CA1 layer of the hippocampus of a coronal brain section. Images of αC labeling (E) and nuclear bis benzimide staining (F) are overlaid (G). No labeling was seen in the negative control without primary antibody (H). Scale bar = 10 μm for E–H. (I–K) Confocal microscopy image of αC labeling in the inner hilar portion of the dentate gyrus of a coronal brain section. Images of

αC labeling (I) and nuclear bis benzimide staining (J) are overlaid (K). Scale bar = 100 μm for I–K. (L–N) Confocal microscopy image of double labeling by αC and αNeuN (1:5K) in the CA1 layer of the hippocampus of a sagittal brain section. Colocalization of αC (L) and αNeuN (M) was consistent with NBCe1-C expression around the pyramidal neurons as seen in the merged image (N). Scale bar = 50 μm for L–N. (O–T) Fluorescence microscopy images of double labeling of αC and αGLAST (1:500) in the hippocampus of a sagittal brain section. Colocalization of αC (O, R) and αGLAST (P, S) in the CA1/CA2 layer (O–Q) and granule layer of the dentate gyrus (R–T) was consistent with NBCe1-C expression in glia as seen in the merged images (Q, T). Scale bar = 10 μm for (O–Q) and 20 μm for (R–T).

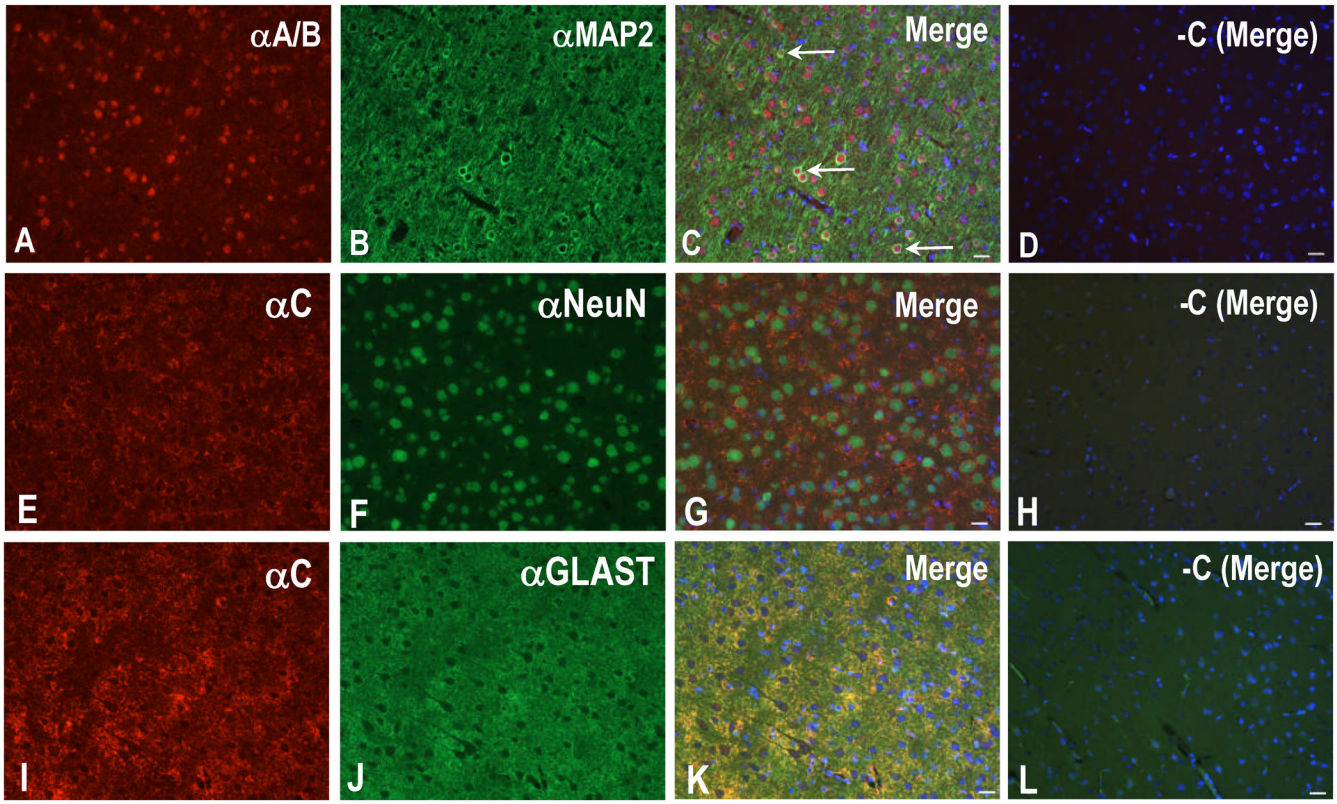

Fig. 8.

NBCe1-A/B and -C expression in the rat cortex. (A–D) Fluorescence microscopy image of αA/B labeling in the cortex of a sagittal brain section. Colocalization of αA/B (A) and αMAP2 (1:100K) (B) was consistent with NBCe1-A/B expression in the cortical neurons as seen in the merged image (C). Strong colocalization was evident in several neurons identified by the white arrows. No labeling was seen in the negative control without primary antibody (D). Scale bar = 20 μm for A–D. (E–H) Fluorescence microscopy image of αC labeling in the cortex of a sagittal brain section. Colocalization of αC (E) and αNeuN (1:5K) (F) was consistent with NBCe1-C expression around the cortical neurons as seen in the merged image (G) No labeling was seen in the negative control without primary antibody (H). Scale bar = 20 μm for E–H. (I–L) Fluorescence microscopy image of distinct αC and αGLAST (1:500) labeling in the cortex of a sagittal brain section. αC (I) and αGLAST (J) colocalized as seen in the merged image (K)— a finding consistent with the presence of NBCe1-C in glia surrounding neurons. No labeling was seen in the negative control without primary antibody (L). Scale bar = 20 μm for I–L.

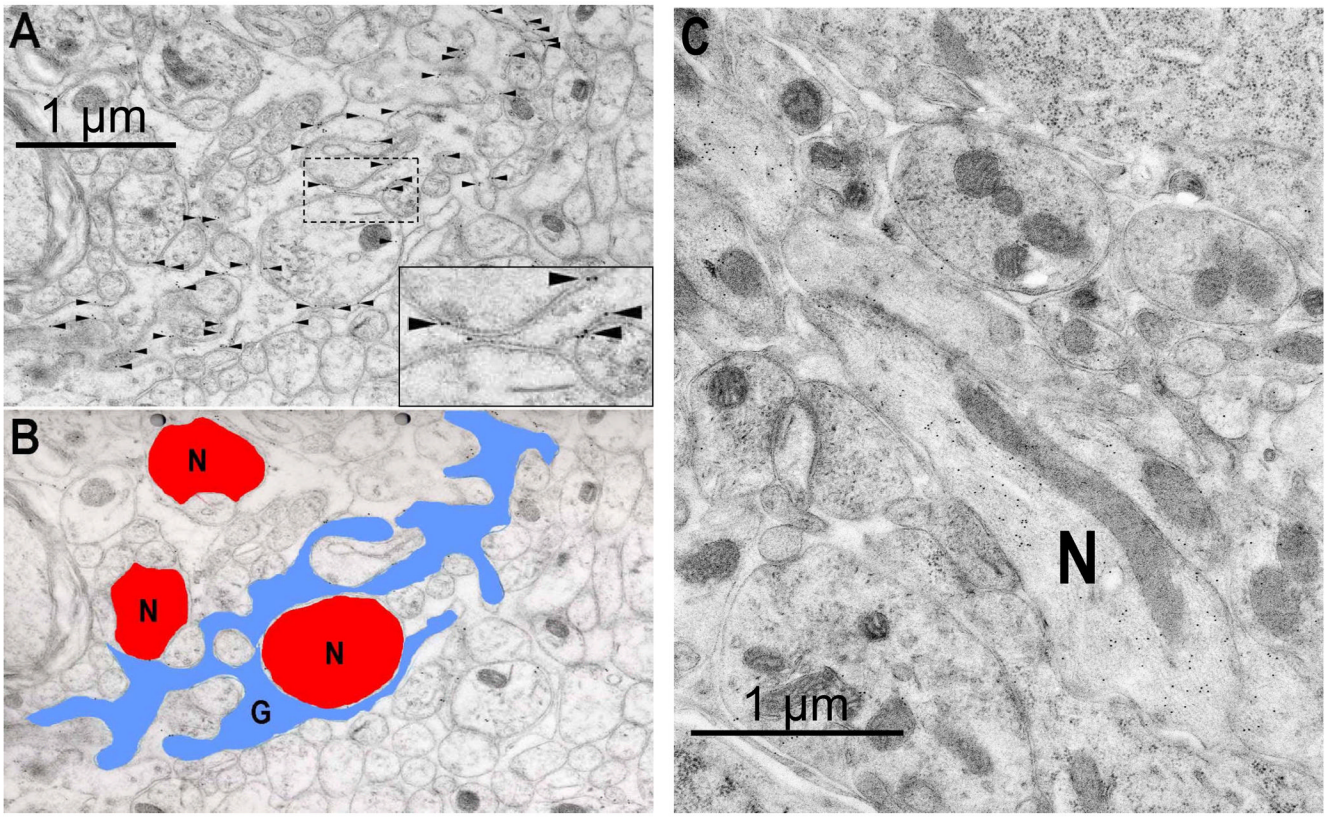

Fig. 9.

NBCe1-C and -A/B expression in the Purkinje layer of rat cerebellum. (A–C) Immunoelectron micrographs demonstrating the subcellular localization of NBCe1-C (A,B) and NBCe1-A/B (C) at the subcellular level. The colloidal gold particles conjugated to the secondary antibody (arrowheads) mark αC labeling of the plasma membrane of a glial cell and are located either directly over or immediately adjacent to the glial membrane profile (A,B). The inset in the bottom, right corner of panel A shows a zoomed-in view of the region identified by the dotted rectangle. This glial cell (G) has a complex shape as illustrated in the cross-section (B) where the cytoplasm is labeled blue. Little or no αC label is associated with adjacent nerve cell profiles (N). In contrast, αA/B is preferentially located in the cytoplasm of some, but not all, nerve fibers (N) observed in the section (C). Scale bar = 1 μm for A–C.